NUMERICAL MODELLING OF FLUID-STRUCTURE INTERACTIONS

A. FORTIN[∗], A. JENDOUBI[∗] AND J. DETEIX[∗]

[∗]GIREF
Département de mathématiques et de statistique
1045 Avenue de la médecine, Université Laval, Québec, Canada, G1V 0A6.
e-mail: afortin@giref.ulaval.ca,
web page: http://http://www.giref.ulaval.ca/accueil.html

Key words: ALE formulation, Moving mesh, Fluid-Structure interactions.

Abstract. Fluid-structure interaction (FSI) problems occur when a potentially deformable solid interact with a surrounding fluid. The flow of the fluid deforms the solid and/or changes its position thus modifying the geometry of the fluid domain. In this paper, we present an Arbitrary Lagrangian Eulerian (ALE) formulation of FSI problems and we present a few numerical examples.

1 INTRODUCTION

Fluid-structure interaction problems occur in various engineering applications and their numerical simulations is still challenging nowadays. Many difficulties arise and we will briefly present some of them in this paper. We consider the general case where the flow of the fluid deforms the solid and changes its position thus modifying the geometry of the fluid domain. Arbitrary Lagrangian Eulerian (ALE) formulations (see [1]) are frequently used to solve such problems where the solid and the fluid are respectively in Lagrangian and Eulerian coordinates. One of the major difficulties in ALE description of fluid-structure interactions is, knowing the displacement of the solid domain, to determine how to update the fluid mesh. If care is not taken, elements adjacent to the solid boundary can degenerate leading to computational problems and eventually to the divergence of the solution process. In this paper, we compare moving mesh methods such as kriging, Laplacian smoothing and displacement methods based on the solution of an elasticity problem. We consider a number of test problems and comment their respective performances.

2 THE COUPLED FSI PROBLEM

2.1 Governing equations

In order to introduce the general non-linear fluid-structure problem, let us consider a time-dependent domain $\Omega(t) \subset \mathbb{R}^d$, $d = 2$ or 3. We assume, for all time t, that $\Omega(t) = \Omega_f(t) \cup \Omega_s(t)$ and $\Omega_f(t) \cap \Omega_s(t) = \emptyset$, where $\Omega_f(t)$ is occupied by an incompressible viscous fluid and $\Omega_f(t)$ by an elastic solid. The reference (initial) configuration of the system is defined $\Omega_0 = \Omega_{f0} \cup \Omega_{s0}$. The fluid-structure interface at time t is denoted by $\Sigma(t) = \overline{\Omega_f(t)} \cap \overline{\Omega_s(t)}$ and $\Sigma_0 = \overline{\Omega_{f0}} \cap \overline{\Omega_{s0}}$ on the initial configuration.

For the fluid, since we are dealing with a moving interface, we consider the incompressible Navier-Stokes equations in ALE formulation (see [2]) :

$$
\begin{cases}
\rho_f \left(\dfrac{\partial \boldsymbol{v}_f}{\partial t} + (\boldsymbol{v}_f - \boldsymbol{v}_{s \mapsto f}) \cdot \nabla \boldsymbol{v}_f \right) + \nabla p - \nabla \cdot \left(2\eta \dot{\gamma}(\boldsymbol{v}_f) \right) &= \boldsymbol{r}_f \ \text{ in } \ \Omega_f(t) \\[2ex]
\nabla \cdot \boldsymbol{v}_f &= 0 \ \text{ in } \ \Omega_f(t) \\[2ex]
\boldsymbol{v}_f(\boldsymbol{x}, t) &= \boldsymbol{v}_s(\boldsymbol{x}, t) \ \text{ on } \ \Sigma(t),
\end{cases}
\tag{1}
$$

where $\boldsymbol{v}_f(x, t)$ is the Eulerian velocity field of the fluid. The vector $\boldsymbol{v}_{s \mapsto f}(x, t)$ is the Eulerian domain (mesh) velocity that will be described later on. As we will see, the domain velocity is naturally defined in the solid domain and must somehow be extended to the fluid domain thus the subscript $s \to f$. Note that in general $\boldsymbol{v}_{s \mapsto f}(\boldsymbol{x}, t) \neq \boldsymbol{v}_f(\boldsymbol{x}, t)$. The continuity of the fluid and solid velocities is imposed on the interface $\Sigma(t)$. The system is completed by initial and boundary conditions on the other parts of the boundary $\Gamma_f^D(t)$ (Dirichlet) and $\Gamma_f^N(t)$ (Neumann). The complete problem is thus defined (and solved) on the current geometry $\Omega_f(t)$.

The motion of the structure is described by the following equations:

$$
\begin{cases}
\rho_{s0} \dot{\boldsymbol{V}}_s - \nabla \cdot \left(\boldsymbol{\Pi}_s(\boldsymbol{U}_s) \right) &= \rho_{s0} \boldsymbol{r}_s \ \text{ in } \ \Omega_{s0} \\[2ex]
\dot{\boldsymbol{U}}_s &= \boldsymbol{V}_s \ \ \text{ in } \ \Omega_{s0}
\end{cases}
\tag{2}
$$

where $\boldsymbol{U}_s(\boldsymbol{X}, t)$ and $\boldsymbol{V}_s(\boldsymbol{X}, t)$ are respectively the Lagrangian displacement and velocity fields of the solid, ρ_{s0} its density in the undeformed geometry and $\boldsymbol{r}_s$ a given body force (usually vanishing). The problem is thus written in a total Lagrangian formulation on Ω_{s0}.

The tensor $\boldsymbol{\Pi}_s = \boldsymbol{\Pi}_s(\boldsymbol{U}_s)$ is the first Piola-Kirchhoff tensor (see Bonet [3]) and is related to the Cauchy stress tensor $\boldsymbol{\sigma}_s$ by the relation:

$$
\boldsymbol{\Pi}_s = J_s \boldsymbol{\sigma}_s \cdot \boldsymbol{F}_s^{-T}
\tag{3}
$$

where $\boldsymbol{F}_s$ is the gradient of deformation tensor and J_s is the Jacobian of the transformation from the initial geometry Ω_{s0} to the current configuration $\Omega_s(t)$. These quantities come

out naturally from the solution of problem (2). This problem is also completed with a proper set of initial and boundary conditions (Dirichlet on Γ_s^D and Neumann on Γ_s^N).

From a mechanical point of view, the coupling between the systems (1) and (2) is realized by imposing the equilibrium of the stresses at the interface:

$$\boldsymbol{\sigma}_s \cdot \boldsymbol{n}_s \; = \; -\boldsymbol{\sigma}_f \cdot \boldsymbol{n}_f \quad \text{on } \Sigma(t),$$

The Cauchy tensor $\boldsymbol{\sigma}_f$ comes out of the solution of system (1) and is defined on the current configuration. System (2) is however solved on the reference configuration. $\boldsymbol{\sigma}_f$ must therefore be transferred on the reference geometry. It is easily seen from (3) and from the transformation of the normal vectors that the above equilibrium condition on the deformes geometry becomes:

$$\boldsymbol{\Pi}_s \cdot \boldsymbol{N}_s = -J_{s\mapsto f}\boldsymbol{\sigma}_f \cdot \boldsymbol{F}_{s\mapsto f}^{-T} \cdot \boldsymbol{N}_f \quad \text{on } \Sigma_0. \tag{4}$$

on the reference geometry. In the above equation, $\boldsymbol{N}$ and $\boldsymbol{n}$ stand for the normal vectors to the initial and deformed geometries respectively. The equilibrium condition (4) is added to system (2) as a Neumann boundary condition. Note that $J_{s\mapsto f}$ and $\boldsymbol{F}_{s\mapsto f}$ are extensions to Ω_{f0} of similar quantities already defined in Ω_{s0}. Their computation will require the definition of a Lagrangian displacement in Ω_{f0}. In practice, any reasonable extension (denoted $\boldsymbol{U}_{s\mapsto f}$) of $\boldsymbol{U}_s|_{\Sigma_0}$ over Ω_{f0} can be used and we will see in Section 3 a number of ways to achieve that goal. It is however quite natural to impose the continuity of the displacements at the interface:

$$\boldsymbol{U}_{s\mapsto f} = \boldsymbol{U}_s \quad \text{on } \Sigma_0 \tag{5}$$

The Lagrangian mesh velocity $\boldsymbol{V}_{s\mapsto f}$ in the fluid domain can then be easily obtained from a finite difference in time. For instance, if an Euler scheme is used, then:

$$\boldsymbol{V}_{s\mapsto f}(\boldsymbol{X}, t) = \frac{\boldsymbol{U}_{s\mapsto f}(\boldsymbol{X}, t+\Delta t) - \boldsymbol{U}_{s\mapsto f}(\boldsymbol{X}, t)}{\Delta t} \tag{6}$$

which, together with (5), imposes the continuity of the velocities on the interface.

We therefore suppose that we have defined an extension $\boldsymbol{U}_{s\mapsto f}$ of the mesh displacement in Ω_{f0} from which we can evaluate $J_{s\mapsto f}$ and $\boldsymbol{F}_{s\mapsto f}$. As a consequence, the current configuration of the fluid domain, $\Omega_f(t)$, is parametrized by:

$$\Omega_f(t) = \Omega_{f0} + \boldsymbol{U}_{s\mapsto f}(\Omega_{f0}) \tag{7}$$

In other terms, each node $\boldsymbol{X}$ of the initial fluid domain has a corresponding node $\boldsymbol{x}$ in the deformed configuration satisfying:

$$\boldsymbol{x} = \boldsymbol{X} + \boldsymbol{U}_{s\mapsto f}(\boldsymbol{X}, t)$$

In this way, we can follow each node of the fluid mesh. Consequently, the Eulerian domain velocity $\boldsymbol{v}_{s\mapsto f}$ at node $\boldsymbol{x}$ satisfies:

$$\boldsymbol{v}_{s\mapsto f}(\boldsymbol{x}, t) = \boldsymbol{V}_{s\mapsto f}(\boldsymbol{X}, t) \tag{8}$$

and will be used in System (1).

3 MESH-UPDATE PROCEDURES

We propose in this section different constructions of the extension $\boldsymbol{U}_{s \mapsto f}$. The main difficulty is to avoid the occurrence of overly distorted elements. Once $\boldsymbol{U}_{s \mapsto f}$ has been constructed, quantities such as $J_{s \mapsto f}$ and $\boldsymbol{F}_{s \mapsto f}$ are easily computed. The mesh velocity is then obtained from (6) and (8). The update of the mesh is thus a crucial step.

3.1 Laplacian smoothing

Laplacian smoothing is a classical method for updating meshes (see [4]). The following problem is solved separately for each component of the displacement.

$$
\begin{cases}
-\Delta \boldsymbol{U}_{s \mapsto f} & = \ 0 \quad \text{in} \ \Omega_{f0}, \\[2mm]
\boldsymbol{U}_{s \mapsto f} & = \ \boldsymbol{U}_s \quad \text{on} \ \Sigma_0, \\[2mm]
\boldsymbol{U}_{s \mapsto f} & = \ 0 \quad \text{on} \ \partial\Omega_{f0} \backslash \Sigma_0,
\end{cases}
\tag{9}
$$

3.2 Elasticity model

Another possibility (see [5]) is to solve the small deformation elasticity system:

$$
\begin{cases}
-\nabla \cdot \left[2\mu \boldsymbol{\gamma}(\boldsymbol{U}_{s \mapsto f}) - \dfrac{2\mu}{3}(\nabla \cdot \boldsymbol{U}_{s \mapsto f})\boldsymbol{I} \right] + \nabla p & = \ 0 \\[2mm]
-\dfrac{1}{k}p - \nabla \cdot \boldsymbol{U}_{s \mapsto f} & = \ 0 \\[2mm]
\boldsymbol{U}_{s \mapsto f} & = \ \boldsymbol{U}_s \quad \text{on} \ \Sigma_0, \\[2mm]
\boldsymbol{U}_{s \mapsto f} \cdot \boldsymbol{n} & = \ 0 \quad \text{on} \ \partial\Omega_{f0} \backslash \Sigma_0,
\end{cases}
\tag{10}
$$

where λ and k (bulk modulus) are obtained from the Poisson coefficient ν and Young's modulus E as

$$
k = \frac{E}{3(1 - 2\nu)} \text{ and } \mu = \frac{E}{2(1 + \nu)}
$$

This problem cannot be solved component per component. It is thus more expensive that the Laplacian smoothing. The value of the Poisson coefficient ν can be chosen close to 0.5 in order to preserve the area (volume) of the elements.

Note also that the last boundary condition allows slip on the boundary nodes which, in some instances, prevents the distortion of elements close to the boundary. It can also be imposed for the Laplacian smoothing if one is ready to solve all the components at the same time.

3.3 Kriging method

Kriging is an interpolation method first introduced by Krige [6] in geostatistics. The displacement is defined as

$$\boldsymbol{U}_{s\mapsto f}(\boldsymbol{X},t) = \sum_{j=1}^{n} \alpha_j g(|\boldsymbol{X} - \boldsymbol{X}_j|) + a_0 + a_1 X_1 + a_2 X_2 + a_3 X_3$$

where the coefficients α_j and a_j have to be determined so that

$$\boldsymbol{U}_{s\mapsto f}(\boldsymbol{X}_j,t) = \boldsymbol{U}_s(\boldsymbol{X}_j,t) \quad j = 1, 2, \cdots, n$$

and to satisfy non-bias conditions (see also Matheron [7]). The function g must be carefully chosen and in this work,

$$g(h) = \begin{cases} h^2 \ln h & \text{for 2D problems} \\ h & \text{for 3D problems} \end{cases}$$

corresponding to a thin shell approximation. It is easily seen that kriging requires the solution of a dense matrix which is still reasonable for two-dimensional applications but quickly becomes prohibitive for three-dimensional ones. More details can be found in Olivier [8]. This approach is also known as the radial basis function interpolation method (see [9]).

3.4 Parabolic smoothing

We propose a slightly modified version of the Laplacian smoothing.

$$\begin{cases} k_0 \boldsymbol{U}_{s\mapsto f} - \Delta \boldsymbol{U}_{s\mapsto f} &=& 0 & \text{in } \Omega_{f0}, \\[2mm] \boldsymbol{U}_{s\mapsto f} &=& \boldsymbol{U}_s & \text{on } \Sigma_0, \\[2mm] \boldsymbol{U}_{s\mapsto f} &=& 0 & \text{on } \partial\Omega_{f0}\backslash\Sigma_0, \end{cases} \tag{11}$$

where k_0 is a constant coefficient chosen large ($k_0 \simeq 500$). In the various two and three-dimensional applications we have considered so far, this is the most robust and the most effective method. Here again, it can be computed for each component separately and very efficient iterative methods exist for this kind of problems so that its solution is not a major issue in terms of computational cost.

4 SOLUTION STRATEGY

The following algorithm is used to solve the global FSI problem. For each time step:

1. Solve the Navier-Stokes equations (1) to obtain the velocity $\boldsymbol{v}_f$, the pressure and the Cauchy stress tensor $\boldsymbol{\sigma}_f$. A mixed formulation (velocity-pressure) is used with a quadratic ($O(h^2)$) Taylor-Hood $P_2 - P_1$ element [10]. The system is solved using a very efficient projection method described in [11].

2. Computation of the right-hand side of (4) and its reinterpolation on the solid side of the interface Σ_0. Note that the meshes in the fluid and solid domains may be non conforming on Σ_0.

3. Solve system (2) to get the solid displacement $\boldsymbol{U}_s$ and velocity $\boldsymbol{V}_s$. A quadratic P_2 element is used for that purpose. Note that a mixed formulation (displacement-pressure) can also be used for incompressible material.

4. Computation of the mesh displacement $\boldsymbol{U}_{s \mapsto f}$ of the fluid domain from the solid displacement field $\boldsymbol{U}_s$ using one of the methods described in Section 3;

5. Update the fluid domain using (7).

6. Compute the mesh velocity $\boldsymbol{V}_{s \mapsto f}$ from equation (6) from which we deduce $\boldsymbol{v}_{s \mapsto f}$.

7. Go back to step 1. if the solution is not converged. Convergence is explicitly verified on each variable of the problem. The norm of the corrections must be smaller than 10^{-8} for all variables before we go to the next time step.

5 NUMERICAL EXAMPLES

We present a numerical example proposed by Turek et Hron [12]. An elastic bar is attached behind a circular cylinder. The vortex shedding behind the cylinder will provoque oscillations of the flexible structure. The geometry is described in the following figure.
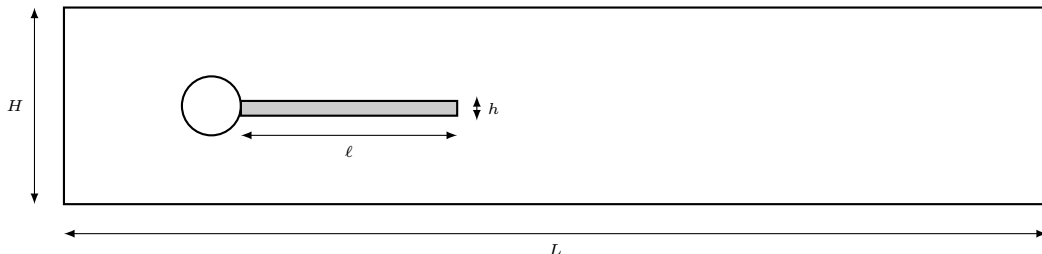
The same dimensions as in [12] were used: $H = 0.41$m, $L = 2.5$m, $h = 0.02$m, and $l = 0.35$m. The cylinder (with radius 0.05m) is centered at $(0.2, 0.2)$. A parabolic velocity profile is imposed at the inlet of the fluid domain as in [12]. The fluid is Newtonian and the solid is modelled using a Saint-Venant-Kirchhoff hyperelastic model

$$\Pi^s = \boldsymbol{F}_s \left(\lambda_s (\operatorname{tr} \boldsymbol{E}) \boldsymbol{I} + 2\mu_s \boldsymbol{E} \right)$$

where $\boldsymbol{E} = \dfrac{\boldsymbol{F}^t \boldsymbol{F} - \boldsymbol{I}}{2}$ is the Green-Lagrange tensor. The parameters for the problem are:

Parameters for the solid	Values	Parameters for the fluid	Valeurs
Density ρ_s [kg $\cdot$ m^{-3}]	10^4	Density ρ_f [kg $\cdot$ m^{-3}]	10^3
Lamé coefficient λ_s [Pa]	2.0×10^6	Kinematic viscosity ν_f [m$^2 \cdot$ s^{-1}]	10^{-3}
Shear modulus μ_s [Pa]	0.5×10^6	Reynold's number Re	100

As an illustration of the displacement methods described in section 3, we present the fluid meshes obtained after a rigid rotation of $\pi/8$ of the structure. Fig. 1 presents the different meshes near the tip of the structure where the displacement is the largest. As can be easily observed, all meshes contain reversed and unusable elements except for the parabolic smoothing method.
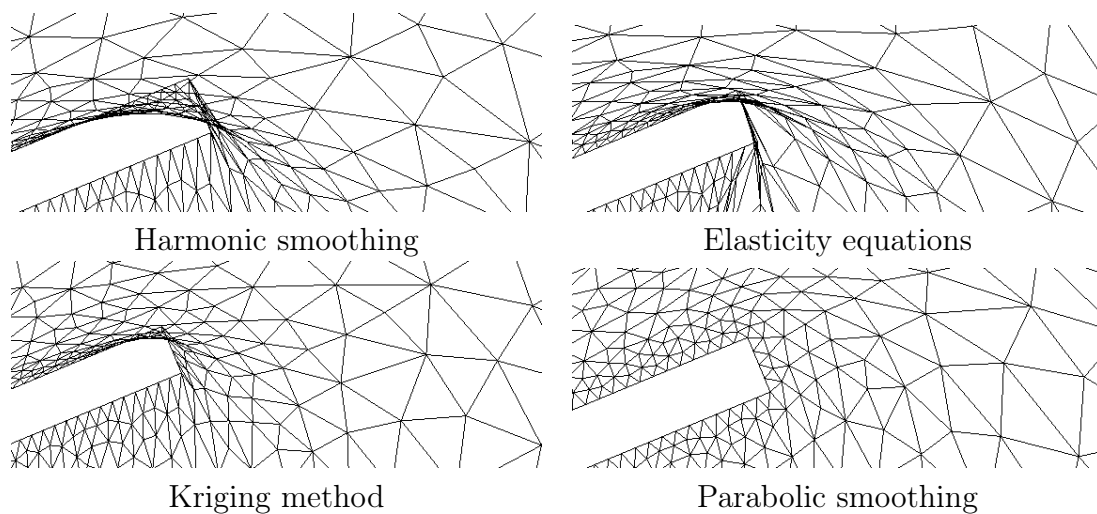

Harmonic smoothing   Elasticity equations

Kriging method   Parabolic smoothing

Figure 1: Mesh displacement

Using thus the parabolic smoothing method, we have successfully solved Turek's benchmark problem. We have been able to reproduce accurately the amplitude end frequency of the displacement of the tip of the structure. Figure 2 shows the velocity field and the position of the structure at three time steps. Note that the kriging method can also be used for the update od the fluid domain. The Laplacian smoothing and the elasticity equations led to reversed elements. Other examples will be presented at the conference including 3D problems.

6 CONCLUSIONS

We have presented in this paper an ALE formulation for fluid-structure interaction problems. In the long term, we are interested in the numerical modeling on aquaplaning which is a major issue in the tyre industry.
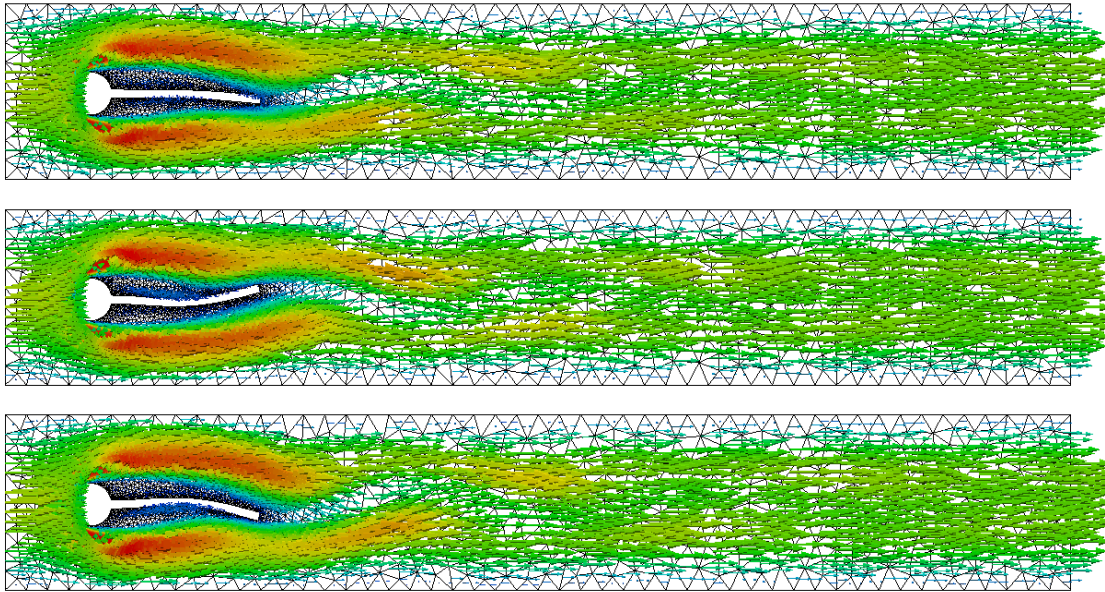
Figure 2: Velocity field and position of the structure

REFERENCES

[1] J. Donea, A. Huerta, J.-Ph. Ponthot, and A. Rodríguez-Ferran. *Arbitrary La-grangian–Eulerian Methods.* John Wiley & Sons, Ltd, 2004.

[2] M.A. Fernández. *Modèles Simplifiés d'Interaction Fluide-Structure.* PhD thesis, University of Paris IX, 2001.

[3] J. Bonet and R. D. Wood. *Nonlinear Continuum Mechanics for Finite Element Analysis.* Cambridge University Press, Cambridge (UK), New York, 2008.

[4] J.U. Brackbill and J.S. Saltzman. Adaptive zoning for singular problems in two dimensions. *J. Comput. Phys.*, 46(3):342–368, 1982.

[5] J.S. Chen, W.K. Liu, and T. Belytschko. Arbitrary Lagrangian–Eulerian methods for materials with memory and friction. In Hughes TJR Tezduyar TE, editor, *Recent developments in computational fluid dynamics*, volume 95, San Francisco, 1988.

[6] D.G. Krige. A statistical method for mine variation problems in the Witwatersrand. *Journal of Chemistry and Metallurgy of the Mining Society of South Africa*, 52:119–139, 1951.

[7] G. Matheron. The intrinsec ramdom functions and their applications. *Advances in Applied Probability*, 5:439–468, 1973.

[8] M. Olivier. *A Fluid-Structure Interaction Partitioned Algorithm Applied to Flexible Flapping Wing Propulsion*. PhD thesis, Département de génie mécanique, Université Laval, Québec, Canada, 2014.

[9] A. De Boer, M.S. Van der Schoot, and H. Bijl. Mesh deformation based on radial basis function interpolation. *Comp. & Struct.*, 85:784–795, 2007.

[10] D. Boffi, F. Brezzi, and M. Fortin. *Mixed Finite Element Methods and Applications*, volume 44 of *Springer Series in Computational Mathematics*. Springer, Berlin, Heidelberg, 2013.

[11] J. Deteix, A. Jendoubi, and D. Yakoubi. A coupled prediction scheme for solving the Navier–Stokes and heat equations. *SIAM Journal of Numerical Analysis*, 52(5):2415–2439, 2014.

[12] S. Turek and J. Hron. Proposal for numerical benchmarking of fluid-structure interaction between an elastic object and laminar incompressible flow. In H.-J. Bungartz and M. Schäfer, editors, *Fluid-Structure Interaction*, volume 53 of *Lecture Notes in Computational Science and Engineering*, pages 371–385. Springer Berlin Heidelberg, 2006.